

Thermal cycling reliability of SnAgCu and SnPb solder joints: a comparison for several IC-packages

Bart Vandeveld, Mario Gonzalez, Paresh Limaye, Petar Ratchev and Eric Beyne
IMEC

Kapeldreef 75, B-3001 Leuven, Belgium

Bart.Vandeveld@imec.be, tel: +32 16 281 513, fax +32 16 281 501

Abstract

This paper deals with a comparison study between SnPb and SnAgCu solder joint reliability. The comparison is based on non-linear finite element modelling. Three packages have been selected: silicon CSP, underfilled flip chip and QFN package. Also the effect of thermal cycling conditions has been investigated. Comparing the induced inelastic strains in the solder joint, the leadfree SnAgCu generally scores better thanks to the lower creep strain rate. On the other hand for the CSP and flip chip package, SnAgCu scores worse for the more extreme loading conditions when the inelastic dissipated energy density is selected as damage parameter. The main reason is that due to the lower creep strain rate, the stresses become higher for SnAgCu resulting in higher hysteresis loops with more dissipated energy per cycle. For the QFN package, SnAgCu scores much better.

1. Introduction

Increasing global concern about the environment is bringing regulatory (European directives) and consumer (“green products”) pressure on the electronics industry in Europe and Japan to reduce or completely eliminate the use of lead (Pb) in products. An important date is July 2006 when Europe forbids the use of lead in electronics.

The transition from a technology using SnPb for electronic interconnections (with more than 50 years of experience) to a new lead-free technology is a challenging and demanding task for the companies. It has an impact on material supply, process equipment and conditions but also the reliability will change. Components have to withstand higher soldering temperatures (typically 20-35°C higher) and the solder joints should have at least the same life time (expressed in number of thermal cycles). This paper only discusses the reliability of the solder joint making the connection with the FR4-board.

W. Engelmaier already mentioned possible appearing problems with leadfree solder joint reliability: “Leadfree solders have creep rates up to 100 times slower than the creep rates of standard Sn/Pb solders. The implication is that meaningful reliability tests cannot be very much accelerated; and that while the use of LF-solder for consumer goods like cell phones is OK, it clearly cannot as yet be recommended for high-reliability applications” [1].

2. Experimental thermal cycling tests of PSGA package

In literature, first results in thermal cycling tests for leadfree-assembled components are published [2-4].

These results depict that there is no general conclusion about the trend in life time from SnPb to SnAgCu. The main conclusion is probably that the trend is very dependent on the package type but also on the applied loading conditions (T_{min} , T_{max} , dwell and ramp-up time). Leadfree solder materials are more creep resistant at high temperatures resulting in higher life time under similar stress conditions for the solder joint. However, the leadfree solder materials have a higher elastic modulus, which can result for certain packages in much higher stress conditions. Moreover, in some packages, the solder joints are subjected to deformations instead of forces (e.g. underfilled flip chip joints) which is often worse for the leadfree solders.

Own experiments with the Polymer Stud Grid Array (PSGA) package [5] have shown that the trend is dependent on the package (Figure 1):

- For the original PSGA package, the reliability of the leadfree assemblies was even lower than for SnPb (SnPb: 6528 cycles; SnAgCu: 5964 cycles).
- For the optimised PSGA package, the reliability of the leadfree assemblies is almost doubled (SnPb: 9160; SnAgCu: 18826). The optimised package differs in the overmould material, which provides a coefficient of thermal expansion (CTE) closer to the one of the package polymer body resulting in lower forces onto the solder joints.

This comparison clearly shows that the trends are dependent on the type of package.

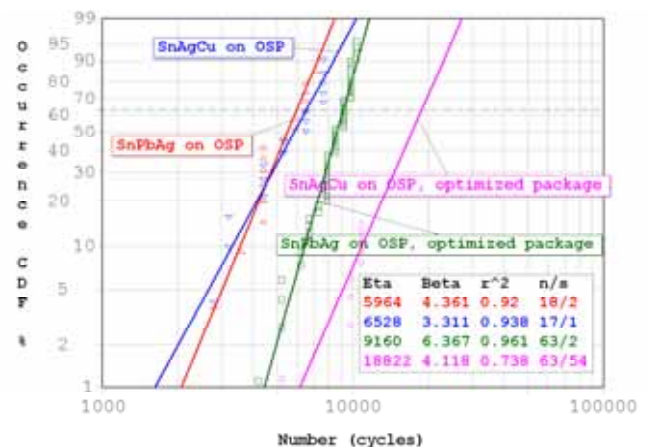


Figure 1: PSGA thermal cycling results (-40 to 125°C, 1 hour cycle time) of original and optimised packages mounted on FR4 board.

A different failure mode is also found for the SnAgCu solder joints [6].

- **SnPbAg:** typical solder fatigue failure is found with the crack propagating along the Sn and Pb grain interfaces (Figure 2).
- **SnAgCu:** also fatigue failure is observed (Figure 3), but the crack propagation is different from the one observed in SnPbAg. The crack propagates through the bulk of the solder in a web-like fashion linking the brittle particles in the solder volume. They are mainly (Au,Ni)Sn₄ particles, if Ni/Au surface finish is used or Cu₆Sn₅ particles, formed with OSP surface finish. The softer Ag₃Sn particles, typical for this solder, do not play a significant role in this process. This failure mode was not observed until now. It is also not clear if the presence of these brittle body particles are positive to the reliability or not. They can initiate cracks but they can also function as crack stoppers or crack deviators. As the tested life time is very high and as we have seen cracks stopping at the particles, we assume that these particles function as crack stoppers/deviators.

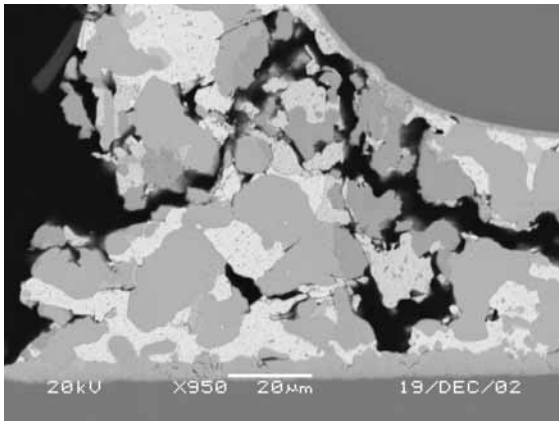


Figure 2: Low magnification SEM picture of a corner SnPbAg solder connection.

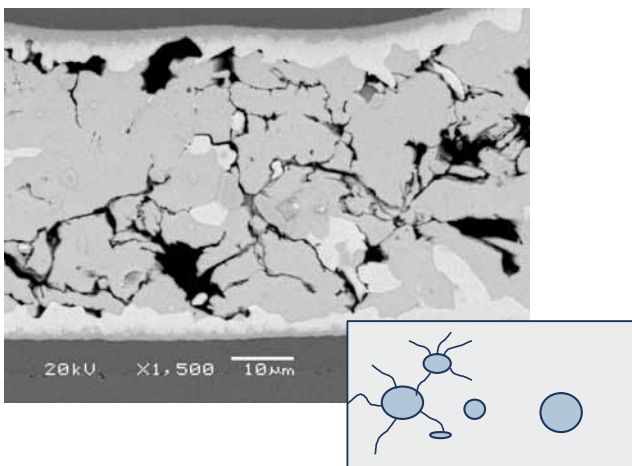


Figure 3: Low magnification SEM picture of a corner SnAgCu solder connection.

3. Material model for SnAgCu compared to SnPb

This section gives the constitutive model for SnPb and SnAgCu, which will be used for the comparison FEM study. Similar to the properties of SnPb, there is also a wide variation in mechanical properties published in literature, with several orders of magnitude differences in creep strain rate values versus temperature and stress. The reasons for the large differences are the sample preparation, the measurement method and probably also the material variation (content of Ag and Cu, which is still not yet standardised). However, all trends show that SnAgCu has a higher elastic modulus and a lower creep strain rate than SnPb.

For this FEM simulation study, we selected following constitutive models.

E-modulus

Following formulae for the elastic modulus have been used:

- SnPb [7]:

$$E = 35366 - 151 \cdot T$$

- For SnAgCu Darveaux proposes to use the SnAg elastic modulus [7]:

$$E = 52400 - 193.05 \cdot T$$

with T in °C, E in MPa.

In this paper, the E-modulus of ref [7] was chosen. A comparative FEM study for several models for E-modulus showed that the difference in the induced strains is only 5% relatively. The induced strains for the model of Lau [8] are slightly higher due to the higher E-modulus at the maximum temperature of the cycle.

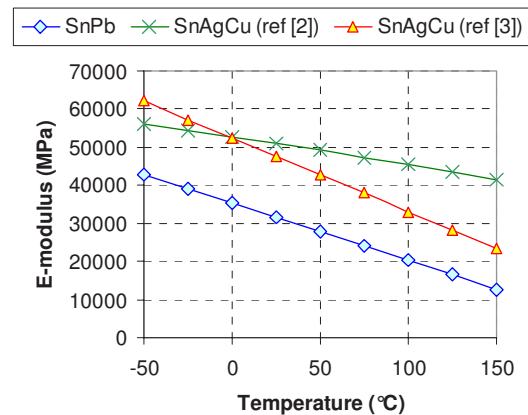


Figure 4: Comparison of elastic modulus for SnPb and SnAgCu, (selected for the FEM simulation for this paper).

Coefficient of Thermal Expansion (CTE):

In literature, we found a realistic CTE value for SnAgCu of 17.6 ppm/°C [4]. This value is significantly lower than for SnPb (25.5 ppm/°C). However, there are also publications showing CTE values up to 21 ppm/°C. The effect of the solder CTE is only on the locally induced stresses and strains.

Yield stress

No good plasticity data for SnAgCu has been found in literature. Some propose to use the data for pure Sn [7], but these yield stress show up to be lower than for SnPb, which is quite unexpected regarding the higher elastic modulus for SnAgCu. Therefore, it was decided to neglect the plasticity behaviour and use **creep as the only inelastic behaviour**. Moreover, the effect of plasticity is negligible [9].

Creep strain constitutive model

The creep material model is important for the simulation. During the last year, several researchers published constitutive models, but there is no generally accepted material model yet. For this study, we selected the model of Wiese, which is based on well-described tests on real size solder joints (no bulk material). The constitutive equations for both solder materials are shown below and are compared in Figure 5 and Figure 6.

- SnPb [7]:

$$\dot{\epsilon} = \frac{6.14 \cdot (76589 - 151 \cdot T)}{T} \cdot \left[\sinh\left(\frac{2027 \cdot \sigma}{76589 - 151 \cdot T}\right) \right]^{3.3} \cdot \exp\left(-\frac{6352}{T}\right)$$

- SnAgCu [10]:

$$\dot{\epsilon} = 2 \times 10^{-21} \cdot (\sigma)^{18} \cdot \exp\left(-\frac{9994.59}{T}\right)$$

with T in K, σ in MPa.

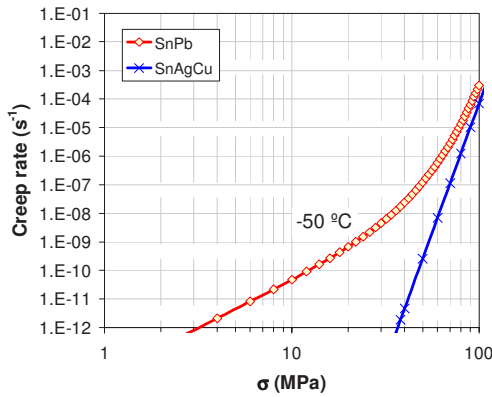


Figure 5: Comparison of creep strain rate vs. Von Mises stress for SnPb and SnAgCu at -50°C (ref [10]).

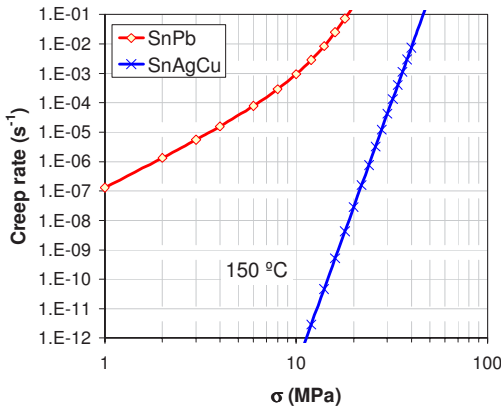


Figure 6: Comparison of creep strain rate vs. Von Mises stress for SnPb and SnAgCu at 150°C (ref [10]).

4. FEM simulation for 5x4 CSP package

The finite element model for the 5x4 CSP package is shown in Figure 7. A uniform temperature cycling load is subjected to the structure and the results of the simulation are the induced deformation and stresses/strains. For this CSP, the main deformation mode of the solder joint is shear between the stiff silicon chip (2.6 ppm/°C, 169 GPa, 0.68 mm thickness) and the FR4 board (16 ppm/°C, 25 GPa, 1 mm thickness). With this model, the one-to-one comparison is simulated for the two solder materials. The simulation is also performed for two loading conditions (Table 1). It is expected that the trends can be dependent on the loading conditions.

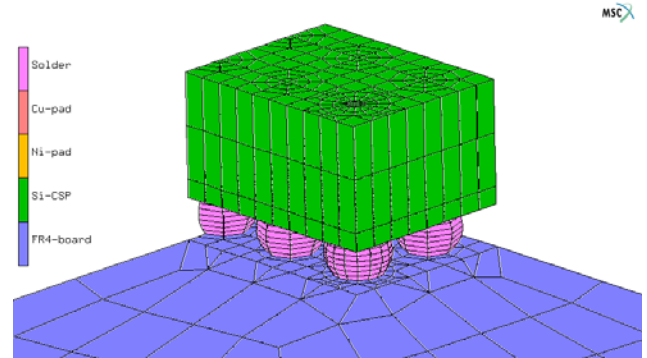


Figure 7: Three dimensional FEM for the 5x4 CSP mounted on a 1 mm thick FR4 board.

Table 1: Three loading conditions for FEM analysis

ID	Range	Cycle time	Ramp-up	Dwell
LC1	0 to 100°C	30 min.	5 min	10 min
LC2	-40 to 125°C	1 hour	15 min.	15 min.

As the thermal mismatch between the chip and FR4 board is linearly dependent on the DNP (distance to neutral point), the highest strains are found in corner joints. Figure 8 and Figure 9 compares the accumulated inelastic strain after two temperature cycles (LC2). The highest strains are in both cases in the corner solder joint and at the chip side. There is no essential difference in strain distribution between the two solders, only the size differs.

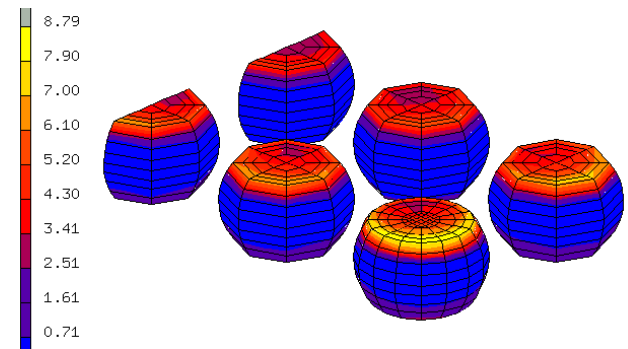


Figure 8: Accumulated inelastic strain in SnPb solder joint after two thermal cycles (LC2).

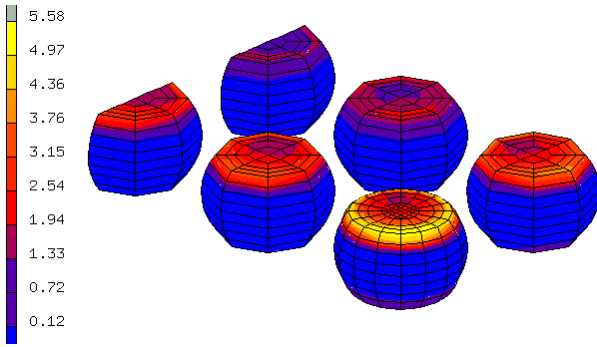


Figure 9: Accumulated inelastic strain in SnAgCu solder joint after two thermal cycles (LC2).

A method of comparing the strain values and to avoid the effects of singularity effects, is to average the strain over a limited number of elements belonging to a damage volume (selected in the area of highest strain). The results of the simulations are shown in Table 2. Following trends are found:

- The strains for SnAgCu are significant higher (2.72x for LC1, 1.66x for LC2). The main reason is the lower creep strain rate for SnAgCu allowing higher stresses before creep occurs.
- The acceleration factor (from LC1 to LC2) is higher for SnAgCu. This includes that more extreme thermal ranges will have more effect on SnAgCu solders (strain increase with factor 2.91 when evolving from LC1 to LC2).

Table 2: Inelastic **strain** per cycle, averaged over damage volume, per thermal cycle for 5x4 CSP package.

Solder	0 to 100°C	-40 to 125°C	Accel. factor
SnPb	1.17 %	2.08 %	AF = 1.78
SnAgCu	0.43 %	1.25 %	AF = 2.91
Pb / Pb-free	2.72	1.66	

Instead of relating the inelastic strain per cycle to expectation of life time, it is also possible to use the induced inelastic energy dissipation. Table 3 shows the results and the conclusion is different from Table 2:

- For LC1, SnPb still scores better than SnAgCu. For LC2, the opposite trend is found. The reason for the different trend in Table 2 vs. Table 3 can be explained as follows. As depicted in Figure 10, the inelastic strain is the width of the stress-strain hysteresis loop achieved in each thermal cycle. The inelastic energy is the area of this hysteresis loop. For SnAgCu, the stresses reach much higher values during the temperature cycling, resulting in higher hysteresis loops. Although the inelastic strain for SnAgCu during LC2 is smaller (= width of the loop), the dissipated energy per cycle (= area in the loop) is higher due to the higher stresses. Figure 11 and Figure 12 shows the hysteresis loops for one normal and one shear stress/strain component and proves the upper statement.

Table 3: Inelastic **energy density** per cycle, averaged over damage volume, per induced cycle for 5x4 CSP package.

Solder	0 to 100°C	-40 to 125°C	Accel. factor
SnPb	0.263 MJ/m ³	0.446 MJ/m ³	AF = 1.70
SnAgCu	0.177 MJ/m ³	0.536 MJ/m ³	AF = 3.02
Pb / Pb-free	1.49	0.83 !!!	

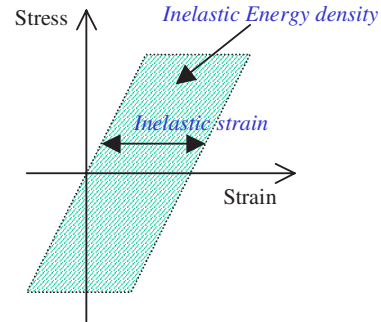


Figure 10: Schematic drawing explaining the difference between inelastic strain and inelastic strain energy density.

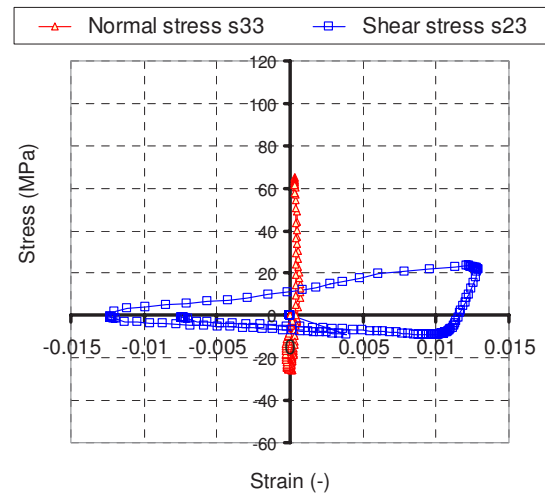


Figure 11: Hysteresis loop for one normal and one shear component for SnPb case

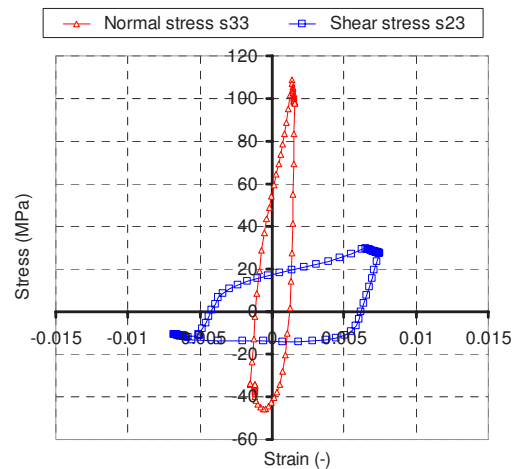


Figure 12: Hysteresis loop for one normal and one shear stress for SnAgCu case.

5. FEM simulation for underfilled flip chip assembly

Figure 13 shows the FEM for an underfilled 5x5x0.68 mm³ flip chip on a 1.6 mm thick FR4 board. An optimised underfill material is used (25 ppm/°C, 10 GPa). The deformation mode for flip chip is significantly different from the CSP. The main load is the out-of-plane thermal mismatch with the underfill [11] instead of shear for the CSP.

Table 4 and Table 5 shows the inelastic strain respectively inelastic energy density for this flip chip assembly. Similar trends as for CSP are found for this structure. In literature, inferior reliability was found for underfilled SnAgCu flip chip, which could be an indication that it is better to look to energy density instead of strain [4].

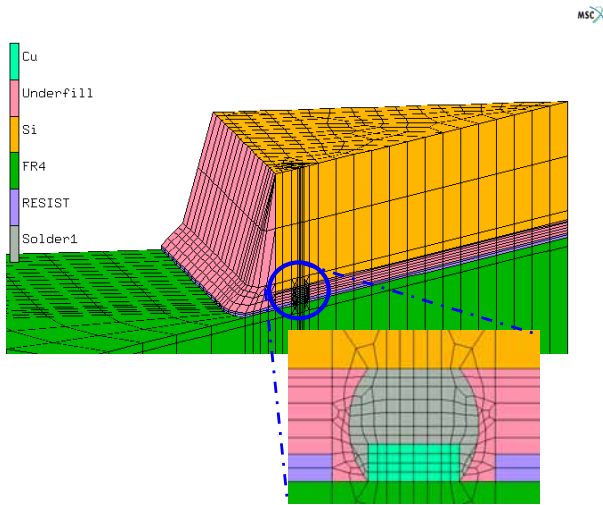


Figure 13: FEM for the underfilled 5x5 mm² flip chip assembly mounted on a 1 mm thick FR4 board.

Table 4: Inelastic **strain**, averaged over damage volume, per thermal cycle for **underfilled flip chip** assembly

Solder	0 to 100°C	-40 to 125°C	Accel. factor
SnPb	1.41%	2.51%	AF = 1.78
SnAgCu	0.73%	1.59%	AF = 2.17
Pb / Pb-free	1.92	1.58	

Table 5: Inelastic **energy density**, averaged over damage volume, per induced cycle for **underfilled flip chip** assembly.

Solder	0 to 100°C	-40 to 125°C	Accel. factor
SnPb	0.340 MJ/m ³	0.510 MJ/m ³	AF = 1.50
SnAgCu	0.311 MJ/m ³	0.700 MJ/m ³	AF = 2.25
Pb / Pb-free	1.09	0.73 !!!	

6. FEM simulation for 56 pins QFN package

The third package that is investigated in this study is the Quad Flat Non leaded (QFN) package, which is nowadays very popular as it is a thermally enhanced package, in particular when the lead-frame is also soldered to the FR4 board.

In this FEM, there is no solder applied in the area between the lead-frame and the PCB. The results are shown in Table 6. When applying SnAgCu, almost no inelastic strains were induced in the solder. The same conclusion is true when analysing the energy density. The main reason is that SnAgCu can support much higher stresses before creep occurs, and it seems that these higher stresses are sufficient to compensate the thermal mismatch between the package and board. For this package, it seems that the lead-free SnAgCu gives a much higher solder reliability than its SnPb alternative.

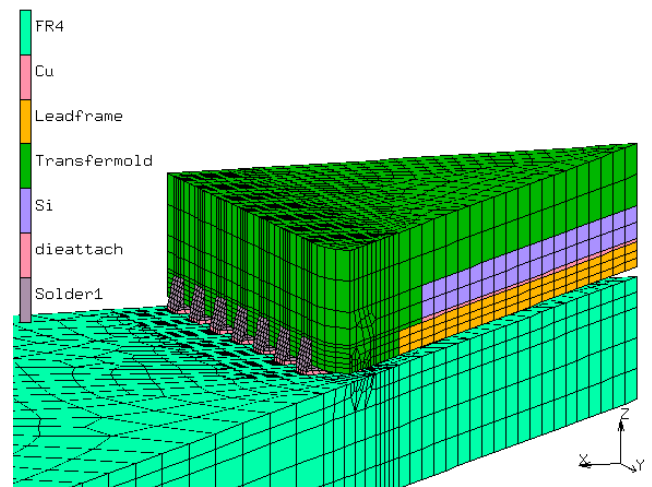


Figure 14: FEM for the 56 pins QFN package assembled to an FR4 board.

Table 6: Inelastic **strain**, averaged over damage volume, per thermal cycle for **56 pins QFN** package

Solder	0 to 100°C	-40 to 125°C	Accel. factor
SnPb	0.44	0.88	AF = 2.00
SnAgCu	0.07	0.19	AF = 2.71
Pb / Pb-free	6.29	4.63	

7. Conclusions

This paper compares the solder joint reliability between two solder materials: SnPb and the leadfree SnAgCu. The comparison is based on non-linear finite element and three relevant packages have been selected: silicon CSP, underfilled flip chip and a QFN package. Also the effect of thermal cycling conditions has been investigated. Comparing the induced inelastic strains, the leadfree SnAgCu generally scores better thanks to the lower creep strain rate. On the other hand for the CSP and flip chip package, SnAgCu scores worse for the more extreme loading conditions when the inelastic dissipated energy density is selected as damage parameter. The main

reason is that due to the lower creep strain rate, the stresses become higher for SnAgCu resulting in higher hysteresis loops with more dissipated energy per cycle. The simulations also show that the acceleration factors for SnAgCu is higher. For the QFN package, SnAgCu scores much better (almost no creep induced).

In thermal cycling tests, we also found a different crack propagation for SnAgCu solders (web-like cracking instead of crack along grains for SnPb).

Experimental results have to prove whether the strain or energy density should be selected as damage parameter. This can be done when sufficient reliability data is available (by internal research activities or in literature).

Acknowledgments

This work has been supported by the EC-Growth GRD1-2001-40712 project with acronym **IMECAT** (www.imec.be/IMECAT).

The authors also would like to thank the people from the ACOSTE and MSR group within IMEC for their support to this paper.

References

- [1] W. Engelmaier, Reliability of leadfree solder joints revisited, Global SMT & Packaging, Nove 2003.
- [2] Bartelo, J., Cain, S. R., Caletka, D., Darbha, K., Gosselin, T., Henderson, D. W., King, D., Knadle, K., Sarkhel, A., Thiel, G. and Woychik, C., "Thermomechanical fatigue behavior of selected lead-free solders", Proceedings, IPC SMEMA Council APEX 2001,
- [3] P. Chalco and E. Blackshear, Reliability issues of BGA packages attached with lead-free solder, Proceedings InterPack01, The Pacific Rim / ASME International Electronic Packaging Technical Conference, July 8-13, 2001, Kauai, Hawaii.
- [4] A. Schubert, R. Dudek, E. Auerswald, A. Gollhardt, B. Michel, H. Reichl, Fatigue Life Models for SnAgCu and SnPb Solder Joints Evaluated by Experiments and Simulation, pp 603-610, ECTC 2003, New Orleans, US.
- [5] A. Chandrasekhar, B. Vandeveld, E. Driessens, E. Beyne, W. De Raedt, P. Pieters, B. Nauwelaers and J. Van Puymbroeck, Modelling and Characterization of the Polymer Stud Grid Array (PSGA) Package: Electrical, Thermal and Thermo-Mechanical Qualification, IEEE transactions on electronics packaging manufacturing, vol. 26, no. 1, pp 54-67, January 2003.
- [6] P. Ratchev, B. Vandeveld and I. De Wolf, Reliability and Failure analysis of SnAgCu solder interconnections for PSGA packages on Ni/Au surface finish, IEEE Transactions on Device and Materials Reliability, Vol. 4, no.1, March 2004.
- [7] R. Darveaux, K. Banerji. "Constitutive Relations for Tin-Based Solder Joints". IEEE Transactions on Components, Hybrids and Manufacturing Technology, 1992, Vol 15, No. 6, Page(s): 1013-1024.
- [8] J. H. Lau, S. H. Pan, C. Chang. "Creep Analysis of Wafer Level Chip Scale Package (WLCSP) with 96.5Sn-3.5Ag and 100In Lead Free Solder Joints and Microvia Build-Up Printed Circuit Board". Journal of Electronic Materials. June 2002, Vol 124, No. 2. Page(s): 69-76.
- [9] B. Vandeveld, E. Beyne, G. Q. Zhang, J. Caers, Solder parameter Sensitivity for CSP Life-Time Prediction using Simulation-Based Optimisation method, Proceedings of the 51st Electronic Components and Technology Conference, pp. 281-287, 29 May - 1 June 2001, Lake Buena Vista, Florida, USA.
- [10] S. Wiese, E. Meusel, K.J. Wolter, Microstructural Dependence of Constitutive Properties of Eutectic SnAg and SnAgCu Solders, proceedings of the 53rd Electronic Components and Technology Conference, 2003, Page(s): 197-206.
- [11] B. Vandeveld, E. Beyne, D. Vandepitte, M. Baelmans, "Semi-analytical model for calculation of induced strains in solder joints of underfilled flip chip assemblies", Proceedings of the 3rd Eurosime conference, pp 86-91, Paris, France, April 14-17, 2002.